A METHOD FOR ESTIMATING DOWNWASH BEHIND SWEPT AIRFOILS

Thesis by

Wilbert G. Wheldon

In Partial Fulfillment of the Requirements

For the Degree of

Aeronautical Engineer

California Institute of Technology

Pasadena, California

1948

ACKNOWLEDGMENT

The author wishes to express his gratitude for the direction and advice given during the preparation of this thesis by Dr. Clark B. Millikan. In addition, appreciation is expressed to Mr. H. A. Storms, Jr., of North American Aviation, Inc., for his suggestion of the topic of the research.

SUMMARY

A theoretical investigation has been made relative to the adaptation of the simple Prandtl wing theory to wings with highly swept lifting lines for purposes of computing downwash. Equations have been developed relating the characteristic geometry of this type of wing to the associated vortex pattern and the Biot-Savart Equation has been integrated in such a way as to most facilitate engineering calculations. The assumption is made that the distribution of circulation about the wing has been predetermined by one of the recently developed span-loading theories.

The general method of approach as has been used by Silverstein, Katzoff and Bullivant in Reference (1) is used herein. The primary deviation from the procedure outlined by these authors is the extension of computational methods from the two dimensional plane-of-symmetry analysis to three dimensions. Though it is not always stated implicitly, some of their devices are employed unchanged and others are altered to fit different conditions.

Calculations have been made (see Appendix A) for a wing for which experimental data on downwash are available. The comparison between theory and experiment is found to be relatively good. Charts and tabular forms have been presented which are expected to be of use to designers interested in tail loads on swept-winged aircraft whose landings and take-offs take place at high angles of attack.

INTRODUCTION

Post-war improvements in jet power plants have extended the maximum speeds at which piloted airplanes may fly. Attempts to push through the so-called "sonic barrier" have recently led aerodynamicists to design wings with radical amounts of sweepback. Much information has been disseminated on the high speed characteristics of these wings but the published literature to date includes very little dealing with the low speed problems associated with their use. These problems, of course, refer to stability and control of the airplane at landing and take-off. A few reports give wind tunnel data of a qualitative nature only on the downwash behind swept wings, but none are known to this writer which correlate these data with theoretical calculations. It is sought with this thesis to fulfill this need for a computational procedure.

Reference (1) sets forth a method, based on the Biot-Savart Law, for finding downwash behind straight wings, with and without flaps, in the region of the tailplane. Application of the Biot-Savart Equation is made comparatively simple by treating the flow as a quasi-two-dimensional problem, that is, the downwash is computed only in the plane corresponding to the wing's plane of symmetry. It ignores the spanwise variation of downwash along the tail, an effect which, as will be shown herein, may be quite pronounced for the new type of wing.

This thesis proposes to adapt to the swept wing the

general methods of these N.A.C.A. authors by assuming the lifting surface to be replaced by a Vee-shaped lifting line. The concept of a vortex pattern composed of a finite number of horseshoe vortices, each of finite strength, is carried over. Consideration is given to those highly complex three dimensional effects which are associated specifically with angle of attack change, effects not present if the lifting line is unbent. The excellent new methods of Weissinger and Falkner (Reference 3) for computing circulation distributions over wings with arbitrary planforms are used for estimating the strengths of the elements of the assumed vortex pattern.

Throughout the preliminary study for the preparation of this paper, consideration was given to various graphical procedures to evaluate their utility in decreasing the tediousness of straight-forward calculations. It was found that in most instances, direct calculations (in tabular form) gave better results at no penalty in time consumption. It appears quite clear that the preparation of downwash charts for wings of various planforms is not amenable to the swept wing. Reference (2), which appeared as a sequel to Reference (1), presented charts for a wide range of planforms but all were of the straight lifting-line variety.

As mentioned in a previous paragraph, for current purposes the spanwise circulation distribution is presumed to be known. However, the methods of Reference (3) are not strictly applicable to wings which have marked discontinuities (such as flaps) in airfoil section or in planform.

Nevertheless, an understanding of the essentials of the problem of flapped airfoils given on page 13, Reference (1), will allow the engineer to make a sufficiently accurate estimate for a swept wing with extended flaps.

NOTATION AND SYMBOLS

x, y, z	Space coordinates measured relative to wind direction with origin at point where quarter-chord lines intersect plane of symmetry of wing
b	Wing span, measured perpendicular to plane of symmetry
c	Wing chord, measured parallel to plane of symmetry
h	Distance from vortex core, measured in the horizontal plane perpendicular to the vortex
m	Linear distance to a point in the flow from the origin of a trailing vortex (at the quarter-chord line), measured parallel to the vortex
mac	Mean aerodynamic chord
n	Length of a given bound vortex filament: $s \sec\varphi$
p	Distance of a point in the flow from the apex of bound vortex filament, measured parallel to the vortex
r	Radial distance of a point in the flow from a given vortex core
s	Distance between wing center plane of symmetry and the parallel plane passing through a given trailing vortex
Δv	Increment of induced velocity at a point in the flow due to the influence of a single vortex filament
w	Downwash velocity
Δw	Increment of downwash velocity due to a single vortex filament
w/V	Downwash angle, radians
AR	Aspect ratio of the wing; b^2/S or $b/c_{average}$
C_l	Local lift Coefficient; (Lift per unit span)/$\frac{1}{2}\rho V^2 c$
C_L	Wing lift Coefficient; (Total lift)/$\frac{1}{2}\rho V^2 S$
S	Wing Area
V	Velocity of the flow in the undisturbed free stream
α	Angle of attack of wing root chord-line relative to undistrubed free stream direction

β	Angle between (1) the line perpendicular to and joining a given vortex filament drawn from a given point in the flow and (2) the horizontal (xy) plane
ϵ	Downwash angle, degrees
Γ	Taper ratio; c_{tip}/c_{root}
$\Delta\Gamma$	Strength of circulation about an individual horseshoe filament
φ	Angle of sweep, measured between the perpendicular to the plane of symmetry and the quarter-chord line, positive if the wing is swept back
ρ	Air density

$(\bar{\ })$	Dimension expressed as ratio of semi-span length; $(\ )/(b/2)$
$(\ )'$	Dimension expressed as a ratio of bound vortex length; $(\ )/(s \sec\varphi)$
$(\ )_L$	Refers to left-hand element of a left-hand, right-hand combination
$(\ )_R$	Refers to right-hand element of a left-hand, right-hand combination
$(\ )_b$	Quantity considered with reference to bound vortices
$(\ )_t$	Quantity considered with reference to trailing vortices

THEORY

PRANDTL SIMPLE WING THEORY:

It is the simple Prandtl wing theory from which have arisen the various methods for calculating spanwise circulation distribution and downwash (as developed by Trefftz, Lotz, Glauert and the more recent authors). This theory visualizes the wing as a straight line in a perfect (non-viscous) fluid coincident with which there is a vortex of varying strength. Since it is known that a vortex filament in a perfect fluid must circle around and close upon itself, it is visualized that vorticity is shed continuously from this "bound" vortex, and that it trails off downstream along those paths that coincide with the streamlines passing through the origins of this vorticity. These trailing filaments ultimately close upon themselves at a great distance downstream, but this distance is so great that the only contributions to the induced field of flow near the wing are (1) from the bound vortex contained in the quarter chord line of the wing and (2) from the trailing vortices which are shed at various spanwise intervals and which trail off past the tail along the paths of the streamlines. The surface containing these infinitesimal shed filaments is known as the "trailing vortex sheet". For purposes of estimating wing load distribution, it is considered that this sheet extends behind the wing and remains as a plane surface which is parallel to the rectilinear flow from infinity.

It is unfortunate that the spanwise circulation distribution (excepting the case of elliptic loading) cannot be represented by a simple analytical expression. This makes it necessary to

employ graphical integrations and stepwise approximations to the circulation curve. For this reason, the concept of "horseshoe" vortices has arisen to enable the aerodynamicist to make calculations for determining downwash. The cross-leg of each horseshoe lies in the quarter-chord of the wing, and the two trailing filaments complete the "U". The loading curve is visualized as a series of finite steps, the one at the tip starting from zero strength. The magnitude of each of these steps is equal to the amount of vorticity shed from the wing within the region extending outboard and inboard midway to the next steps, and it is this amount of vorticity which is the strength of the U filament whose trailing legs originate from their respective sides of the wing at the point.

In the older theories which have been used to find this circulation distribution, it has been found necessary to consider the bound vortex straight and at right angles to the windstream. The reason lies in the fact that infinite velocities theoretically are induced along the lifting line, should it not be perpendicular to the wind. For purposes of computing downwash, however, this consideration does not enter the problem and a swept wing can be considered as a Vee-shaped lifting line in a vortex pattern which is otherwise identical with that which has already been described for the straight wing.

In this thesis, therefore, it will be assumed that the downwash at any position in the flow will be induced (1) by a finite number of coincident bent filaments lying in the quarter-chord of the wing, and (2) by a set of trailing vortices, all

lying in the surface which originates at the lifting line. Attention will be given to the effect of reorienting this pattern (as the wing changes angle of attack) upon the downwash.

DEVELOPMENT OF THE EQUATIONS FOR DOWNWASH:

The velocity induced at a point in the field of flow due to an infinitesimal length of vortex filament, $d\bar{w}$, is expressed by means of the Biot-Savart Law as

$$d\bar{w} = \frac{\Gamma}{4\pi} \frac{d\bar{\ell} \times \bar{a}}{|\bar{a}|^3} \qquad (1)$$

The quantities appearing herein are defined:

$\bar{w}$ ~ induced velocity vector at the given point

Γ ~ strength of circulation about the vortex

$d\bar{\ell}$ ~ direction vector of the small length of vortex filament

$\bar{a}$ ~ vector from the filament to the given point

This equation will be integrated (1) to obtain the field of induced velocities due to a single leg of the Vee portion of the horseshoe vortex emanating from a swept-wing, and (2) to find the induced field due to the singly-infinite trailing portions of the horseshoe. The vectors representing the velocities obtained from the procedure will lie in the plane normal to that part of the filament from which they were derived. By suitable geometrical methods the vertical components of these induced velocities will be extracted, and a method will be given to compute and to sum all the contributions from the several vortices of the vortex system.

See Figure (1) for a sketch defining quantities involved in the integration procedure.

To find the induced velocity, Δv, occuring at point P due to the vortex of length n (= s sec φ) depicted above, we write $d\bar{\ell} \times \bar{a} = a \sin\theta \, d\ell$, substitute into the Biot-Savart

Equation and integrate between the limits $0 \leq \ell \leq n$.

$$\Delta v\left(\frac{4\pi}{\Gamma}\right) = \int_0^n \frac{a \sin\theta \, d\ell}{a^3} = r_b \int_0^n \frac{d\ell}{\left[r_b^2 + (p-\ell)^2\right]^{3/2}}$$

$$= \frac{1}{r_b}\left[\frac{\ell - p}{\sqrt{r_b^2 + (p-\ell)^2}}\right]_0^n = \frac{1}{r_b}\left[\frac{n-p}{\sqrt{r_b^2 + (p-n)^2}} + \frac{p}{\sqrt{r_b^2 + p^2}}\right] \qquad (2)$$

By a similar procedure, the incremental induced velocity from the trailing vortices at a point whose distance normal to the vortex is r_t and which is distant m units downstream from the vortex corner is

$$\Delta v\left(\frac{4\pi}{\Gamma}\right) = \frac{1}{r_t}\left[\frac{\ell - m}{\sqrt{r_t^2 + (m-\ell)^2}}\right]_0^{\infty} = \frac{1}{r_t}\left[1 + \frac{m}{\sqrt{m^2 + r_t^2}}\right] \qquad (3)$$

A semi-graphical solution will be followed in determining the vertical component of the induced flow, i.e., the downwash. To do this, a system of coordinates is established as shown in Figure (2).

Concerning ourselves again with the bound vortices, if each of the distances involved is expressed dimensionlessly in terms of the bound vortex length, $s \sec\varphi$, then a single graph may be prepared from which the quantity $\Delta v\left(\frac{4\pi}{\Gamma}\right)$ may be found for all values of r_b' ($= r_b / s \sec\varphi$) and of p' ($= p/s \sec\varphi$). Making these substitutions in Equation (2)

$$\Delta v\left(\frac{4\pi}{\Gamma}\right) = \frac{1}{(r_b)(b/2)}\left\{\frac{1-p'}{\sqrt{r_b'^2 + (p'-1)^2}} + \frac{p'}{\sqrt{r_b'^2 + p'^2}}\right\} \qquad (4)$$

The vertical component of Δv may be determined by multiplying this Δv by the cosine of the angle between the horizontal and the radius from the vortex to the point P. This cosine is

invariant with the length of the Vee leg of the vortex. Therefore,

$$(w/V)_b = \cos\beta_{b_R}\sum\left[\left(\frac{1}{4\pi}\right)\left(\frac{2\Gamma}{bV}\right)\left(\frac{1}{\bar{s}\,Sec\,\Phi}\right)\left(\frac{1}{r'_{b_R}}\left\{\frac{1-p'_R}{\sqrt{r'^2_{b_R}+(p'_R-1)^2}}+\frac{p'_R}{\sqrt{r'^2_{b_R}+p'^2_R}}\right\}\right)\right]$$
$$+\cos\beta_{b_L}\sum\left[\left(\frac{1}{4\pi}\right)\left(\frac{2\Gamma}{bV}\right)\left(\frac{1}{\bar{s}\,Sec\,\Phi}\right)\left(\frac{1}{r'_{b_L}}\left\{\frac{1-p'_L}{\sqrt{r'^2_{b_L}+(p'_L-1)^2}}+\frac{p'_L}{\sqrt{r'^2_{b_L}+p'^2_L}}\right\}\right)\right] \qquad (5)$$

where the terms $2\Gamma/bV$ represent the strengths of the shed and bound vortices as determined from the spanwise circulation distribution.

A graph of the function

$$F_b = \frac{1}{r'_b}\left\{\frac{1-p'}{\sqrt{r'^2_b+(p'-1)^2}}+\frac{p'}{\sqrt{r'^2_b+p'^2}}\right\}$$

is presented as Figure (8).

Regarding the trailing vortices, the distances are expressed as ratios of the wing semi-span distance b/2. This puts Equation (3) in the form

$$\Delta v\left(\frac{4\pi}{\Gamma}\right) = \frac{1}{\bar{r}_t\, b/2}\left\{1+\frac{\bar{m}}{\sqrt{\bar{m}^2+\bar{r}_t^2}}\right\} \qquad (6)$$

As in the previous case, to convert this velocity to its vertical component one must multiply it by the cosine of the angle which the radius through point P normal to the vortex makes with the horizontal. This cosine will not in general be the same for various trailing vortex positions. Hence,

$$(w/V)_t = \sum\left[\left(\frac{1}{4\pi}\right)\left(\frac{2\Gamma}{bV}\right)\right]\left[\cos\beta_{t_R}\left\{\frac{1}{\bar{r}_{t_R}}\left(1+\frac{\bar{m}}{\sqrt{\bar{m}^2+\bar{r}_{t_R}^2}}\right)\right\}\right.$$
$$\left.+\cos\beta_{t_L}\left\{\frac{1}{\bar{r}_{t_L}}\left(1+\frac{\bar{m}}{\sqrt{\bar{m}^2+\bar{r}_{t_L}^2}}\right)\right\}\right] \qquad (7)$$

The function $F_t = \frac{1}{\bar{r}_t}\left(1+\frac{\bar{m}}{\sqrt{\bar{r}_t^2+\bar{m}^2}}\right)$ appears as Figure (9).

GEOMETRICAL COMPLICATION

The downwash theory used with straight lifting lines need give no consideration to changes in the vortex pattern which result solely from changes in angle of attack. But whenever the attitude of a swept wing is changed, each component vortex of the pattern is translated and the lifting vortex is rotated about the pitching axis. Much complication arises from rotation of the "Vee" vortex since the calculation of downwash induced by it involves computing the length of the normal to a line in space which is neither parallel to any of the established axes nor to any of the x = constant, y = constant, or z = constant planes; and it involves in addition finding the cosine of the angle this normal makes with the horizontal.

To find relationships giving the radii, r_b, of a point in space from either leg of the "Vee" vortex, one must consider the geometry of a given plane. It rotates about the y axis and makes an angle α with the x axis. The "Vee" lifting line is contained in this plane and its legs form the angle φ with the positive and negative branches of the y axis.

The desired relations for the radii are found to be expressed by

$$\bar{r}_{b_R} = \sqrt{(K\cos\varphi - \bar{Y}\sin\varphi)^2 + J^2}$$
$$\bar{r}_{b_L} = \sqrt{(K\cos\varphi + \bar{Y}\sin\varphi)^2 + J^2} \qquad (8)$$

where

$$J = \bar{X}\sin\alpha + \bar{Z}\cos\alpha$$
$$K = \bar{X}\cos\alpha - \bar{Z}\sin\alpha$$
$\bar{X}, \bar{Y}, \bar{Z}$ ~ coordinates of the point.

The corresponding dimensionless quantities giving the longitudinal distances of the point from the origin (measured parallel to the two legs of the "Vee") are

$$\begin{aligned} \bar{\rho}_R &= K \sin\varphi + \bar{Y}\cos\varphi \\ \bar{\rho}_L &= K \sin\varphi - \bar{Y}\cos\varphi \end{aligned} \tag{9}$$

If β is the angle that the horizontal through the point makes with the radius, then

$$\begin{aligned} \cos\beta_{b_R} &= \frac{1}{\bar{r}_{b_R}}\sqrt{(\bar{Y} - \bar{\rho}_R\cos\varphi)^2 + (\bar{X} - \bar{\rho}_R\sin\varphi\cos\alpha)^2} \\ \cos\beta_{b_L} &= \frac{1}{\bar{r}_{b_L}}\sqrt{(\bar{Y} + \rho_L\cos\varphi)^2 + (\bar{X} - \bar{\rho}_L\sin\varphi\cos\alpha)^2} \end{aligned} \tag{10}$$

Thus, to find the downwash at the point, knowing the magnitude of the total induced velocity at that point, one employs the expression

$$\Delta w_{b_{R,L}} = \Delta v_{b_{R,L}} \cos\beta_{b_{R,L}} \tag{11}$$

which is to be compared to Equation (5).

DISTORTION OF THE VORTEX SHEET - GENERAL DISCUSSION

One of the more important of the deviations of the downwash picture from the initial assumptions is the phenomenon of "rolling-up" of the vortex sheet. Were there to be no bound vortex and but a single trailing vortex filament shed from the lifting line, it would trail off downstream following the rectilinear flow streamline passing through its point of inception. Other streamlines in the region would be bent from parallel paths due to its influence but this one vortex would remain straight. However, since not just one but an entire sheet made up of these vortices exists, the mutual induced velocities acting upon one another cause the paths of all of them to be changed. Each vortex path coincides with that of a streamline, so it can be seen that as the streamlines bend under the influence of the induced velocities, the entire sheet must become warped.

Consider a straight lifting line from which just two trailing vortices are shed near each tip. The vortex sheet (of four vortices) must roll up, concave upward. The velocities from the outboard cores force the paths of the inner cores downward; those from the inner cores displace the outer ones upward. Refer to Figure (3), which illustrates the fact that the inner cores are forced downward and outboard a distance which exceeds the upward and inward motion of the others. This is the result of the greater magnitude of vorticity which exists at the tips of a swept-back wing relative to that shed nearer the center of the wing.

We next consider a swept lifting line at some angle of

attack to the free stream. With no vorticity emanating from this line, the sheet of streamlines passing the line will appear downstream as an inverted trough-shaped surface. The apex of the trough for a swept-back line will be directed upward, and were the angle of attack to be increased to 90^{o}, the trough half-angle would correspond to the sweep angle. For a swept-forward line, the apex would point downward.

The addition of circulation to the elements of the trough will once again superimpose a rolling-up upon the outer edges of its surface. For the two-horseshoe pattern previously discussed, the more inward streamlines are displaced downward a distance relatively greater than they are in the straight lifting line case. This arises from two phenomena associated only with sweepback. First, the tip vortices from swept-back wings have abnormally high values of circulation. The relative strengths of the induced velocities in the region of the cores located a small distance inboard from the tips are, therefore, greater than those further outboard. Second, since the downward displacement of any streamline which passes through the lifting line is a function (a) of the downwash acting along its length and (b) of the distance along its path, the longer the path, the greater the displacement. But the outer streamlines must traverse a shorter path to their intersection with any x = constant plane since their point of origin on the swept-back lifting line is farther downstream. See Figure (4). These two phenomena combine to displace the inboard elements of the vortex sheet further from the line paralleling the free-stream direction.

This rolling-up is then superimposed upon the inverted trough pattern to give the configuration of the intersection of the wake with any plane normal to the free flow.

The same type of reasoning may be applied to the swept-forward lifting line, remembering that for this case the vorticity shed near the center of the Vee, rather than that near the tips, is stronger and that the tip vortices travel a longer, rather than shorter, path to the plane of interest.

It is of importance to consider the treatment of the problem of vortex sheet distortion given in Reference (1). Figure (12) of this reference is roughly reproduced in Figure (5) of this report, in which the variation of downwash with vertical distance from the wing quarter-chord point for a straight USA 45 airfoil is plotted at the plane of symmetry for three cases. Curve (b) of this figure gives the downwash computed on the assumption that the trailing vortex sheet remains plane as the flow progresses downstream to infinity. Curve (a) is computed on the basis of a distorted vortex sheet, concave upward (see the auxiliary figure). Noticing that for this case the two curves were geometrically similar, the authors implicitly concluded that satisfactory computational accuracy could be obtained for the type of wing they were considering if the downwash pattern existing in any plane downstream from the wing perpendicular to the rectilinear flow were shifted downward by the distance "z" shown in the auxiliary figure. This reference makes the assumption that the downwash (for a straight wing) is nearly constant across the tail span. Actually, a procedure having common use in the industry makes

use of the downwash data of References (1) and (2) by assuming the effective downwash acting at the elevator hinge line to be nine tenths of that computed to exist at the center of the tail. This procedure yields results which are approximately correct in the plane of symmetry, but large discrepancies may result from applying it to the flow near the horizontal stabilizer tips. This is illustrated in Figure (6). If $\overline{CDE}$ represents the elevator hinge line of a horizontal tail in the flow depicted, then it is seen that at point C at the stabilizer tip the downwash induced by the vortex at A is (in this case) more than double the magnitude of that from the vortex of equal strength at B. But at point D, the downwash increments from the two tip vortices at A and B are about equal. Relative to those vortices located at points approaching point F along each of the two sheets, it is seen that the downwash increments approach each other in magnitude. Assuming that in the more conventional type of aircraft the horizontal tail will lie above the vertical position of the tip vortices, the greater the distortion of the vortex sheet, the greater will be the error made in assuming a flat vortex sheet passing through point F.

DETERMINING THE SHAPE OF THE VORTEX SHEET:

For reasons just described it becomes necessary to know the positions of the various elements of the vortex pattern relative to the points at which downwash is being computed. This requires a knowledge of the distorted shape of the vortex sheet, a shape which generally will vary a great deal from that of a plane area. Because of inherent difficulties arising from the three dimensional geometry involved, no precise mathematical analysis of the problem can be made. Certain simplifying assumptions, however, allow an approximate procedure which is justified by various experimental investigations.

Briefly, the process involves computing the downwash induced by the entire system along two or three of the finite trailing vortices which were taken to replace the continuous distribution. This establishes the paths of these filaments; each must follow the course of the streamline through its origin, and the inclination of the streamline at any point is determined by the direction of the vector-sum of the free stream velocity plus the local induced velocity. The assumption is made that sidewash is negligible so that the path of the vortex remains always within the plane $\bar{y} = \bar{s}$.

The first approximation to the vertical location of the vortex sheet is the basic one, i.e., that the trailing vortices remain parallel to the free stream velocity. Integration of the downwash angle along a vortex from its origin to any value of $\bar{x}$ gives the vertical displacement of the streamline containing that vortex, i.e.,

$$\bar{z} = -\int_0^{\bar{x}} \frac{w}{V} d\bar{x} + \bar{z}_{\text{vortex origin}} \qquad (12)$$

From the above equation the positions of all points through

which the particular vortices pass can be found, and it is then possible to plot the intersection of each with any plane perpendicular to the free stream direction downstream from the wing.

The best assumption as to the vertical position of the trailing vortex origin must be largely a matter of judgment. It depends upon angle of sweep, angle of attack, extension of flaps, separation of flow along the wing's upper surface, and upon the distance of the trailing edge from the lifting line. Reference (1), page 17, contains an excellent procedure for locating this point. In general, the vortex origin will be in the neighborhood of the median between the upper surface of the laminar flow separation region and the trailing edge of the flap or wing.

CALCULATION OF DOWNWASH:

The mathematical process leading to the determination of downwash at a point behind a wing having a swept lifting line takes place in three distinct steps. The first is that of finding the distribution of circulation along the span of the wing. Methods for carrying this out are beyond the scope of this paper. The next step includes the approximation to the actual continuous distribution of vorticity by a pattern of Vee shaped horseshoe vortices, and the determination to the first order of accuracy of the distortion of that pattern under the influence of its own induced velocities. In the final step, having assumed a vortex pattern whose shape is similar to that found by the latter part of step two, the downwash is calculated at the desired points in the field of flow.

- - - - - - - - - - - - - - - - -

1. Compute for the given wing at the given lift coefficient the circulation distribution about the quarter chord line. Use either the Weissinger lifting line method or the Falkner lifting surface method. The former is much the preferable for downwash purposes since the results are obtained with considerably less effort and, for general spanwise circulation distribution, are just as accurate. Determine $dC_L/d\alpha$ and the angle of attack corresponding to the given C_L.

2. Assume a vortex pattern and compute the distortion of the trailing vortex sheet to the first order approximation.

   a. Replace the continuous vorticity distribution by a finite number of horseshoe filaments. The strength of each filament is given by the difference in circulations

around the lifting line between (1) the point at which its trailing leg leaves the wing and (2) the point on the wing where the next inboard filament is shed. The sum total of the strengths of the individual vortices must equal the total quantity of vorticity under the spanwise distribution curve. See Figure (7).

b. Assume the vortex sheet to be undistorted. That is, assume that there are no induced velocity effects acting on the component trailing vortices of the assumed pattern. The sheet will appear as an inverted trough (for a wing with positive angles of attack and sweep).

c. Locate the origins of the trailing vortices. The section entitled "Location of the Wake", Page 17, Reference (1), presents a semi-empirical approach to this problem. (The vortex sheet and the center of the wake are coincident; they have a common origin and are equally free to move in the induced velocity field behind the wing). If the wing has a trapezoidal planform with only moderately rounded tips, the location of the point at which the trailing edge of the wing intersects the vertical plane containing any given trailing vortex filament is given by

$$\bar{X}_{T.E.} = \bar{s}\cos\alpha\left\{\tan\varphi + \frac{3}{AR}\left(\frac{1-\lambda}{1+\lambda}\right)\right\} + \frac{3}{AR}\frac{\cos\alpha}{1+\lambda}$$

$$\bar{Z}_{T.E.} = -\bar{s}\sin\alpha\left\{\tan\varphi + \frac{3}{AR}\left(\frac{1-\lambda}{1+\lambda}\right)\right\} - \frac{3}{AR}\frac{\sin\alpha}{1+\lambda} \qquad (13)$$

d. An element of the vortex sheet follows a path whose tangent at any point takes the direction of the vector sum of the induced and the free stream velocities. So in this

step, compute the downwash due to the field assumed in Step b along three or four points on certain of the streamlines which lie within the vortex sheet. Inasmuch as the curvature of the sheet will be greatest near the tips, it will be satisfactory to make these calculations for only two or three of the streamlines near the tip and for the single streamline lying in the plane of symmetry of the wing. Normally, one is not interested in the field of flow further downstream than the vertical plane through the elevator hinge line. Therefore, the three or four points on the individual streamlines should include (1) the origin of the vortex (at or near the wing trailing edge), (2) the point where the streamline intersects the plane of interest (elevator hinge line plane) and (3) a point or two spaced nearer to the origin than to the tail, for it is in this region that the greatest curvature of the streamlines will occur.

e. Prepare a plot of downwash angle versus linear distance downstream from the vortex origin for each of the streamlines of Step d. The displacement vertically downward of any point on a streamline is given by Equation (12). This integral may be evaluated by Simpson's rule or by other approximate methods. Carry out the integration downstream as far as the elevator hinge plane. From the results of this step, prepare another plot of $\bar{z}$ versus $\bar{s}$ in the elevator hinge plane. The curve through the points of this plot represents to a first approximation the intersection of the distorted vortex sheet with the plane of interest.

3. Finally, we may calculate the downwash in the plane of interest along the elevator hinge line (if, as is ordinarily the case, downwash at the horizontal tail is of primary interest to the aerodynamicist). The vortex pattern is now composed of the bound vortices, located as before in the wing quarter chord line, plus the spanwise distribution of trailing vortices. Each of these lies in the same spanwise plane as before, but is assumed to have been translated downward parallel to the x axis to a position passing through the curve computed by Step 2(e).

Judgment must be exercised when making a choice of points along the tailspan for finding the downward flow. In the vortex sheet behind an actual wing the vortices are all of infinitesimal strength (with the exception of the tip vortex of a sheet which has undergone complete rolling up). But under our assumption of finite-strength filaments, velocities bordering on the infinite can exist at very small distances from the vortex. For this reason it is necessary to avoid making calculations at any point close to one of these. If the downwash is desired in the region of the vortex sheet, a satisfactory choice of points is either (1) midway between two adjacent cores, or (2) along the vertical line drawn through any one of them. The latter choice has the virtue that no matter where the point may be up or down along the line, that particular core contributes nothing to the downward induced velocity there and can be neglected.

Two simplifying procedures may sometimes be employed for calculating the effect of the bound vortex in the plane of interest. First, the downwash induced by it at any spanwise point on the sheet may be assumed to remain constant for small distances

above and below the sheet. This makes certain of the w_B data computed in Step 2(d) available for use in this step. Second, if the vertical dimension between a given point and the mean height of the Vee filaments is small, the cosine of the angle can be taken as unity. Both of these simplifications owe their validity to the magnitude, usually small, of the downwash coming from the lifting line in the region of the tail. Their use is the more justified, the further back is the plane of interest from the wing.

RESULTS AND DISCUSSION:

The methods of the foregoing analysis have been applied to a wing for which experimental data are available, the calculations having been included in Appendix A. The wing, a full scale airfoil, was of low aspect ratio (3.64) and was highly swept ($\varphi = 45^{\circ}$). The downwash surveys were made in a full scale tunnel, the Reynolds Numbers of the tests comparing closely with those likely to be encountered in actual flight.

Unfortunately, since the experimental data appear in a report having a government security classification, they cannot be reproduced in this thesis.

The final results of the procedure, i.e., the calculated downwash in a plane 2.75 semispans downstream from the 25% point on the m.a.c., appear in Figure (15). The computed values are few in number since time prevented a more exhaustive study. In order to approach the problem from the designer's viewpoint, the calculations were carried out at the same C_L as for the experimental surveys but at an angle of attack of 15.1 degrees as computed from the theoretical $dC_L/d\alpha$ (.047 per degree). This angle exceeded by two or three degrees the experimental value, the theoretical being lower than the experimental lift curve slope. The errors introduced into the method herein show up as a slight overdistortion of the vortex sheet.

The comparison between theoretical and experimental results may be taken as justification of the use of the method, and can be stated to be:

(a) The prediction of the wake centerline for this case is nearly perfect.

(b) Above and below the wake centerline, the computed downwash is somewhat low (roughly, ten to twenty percent).

(c) The predicted values of downwash along the wake centerline are close to the experimental values.

Result (a) of the above comparison leads to the conclusion that the position of the wake may be located theoretically with good accuracy. It is seen that a two or three degree error in angle of attack prediction probably does not introduce overly adverse results.

It is thought that result (b) can be attributed to the differences between the actual span load distribution and the theoretical value taken from Reference (3). The theoretical methods for computing circulation are all based on a procedure which presumes that the slopes of the airfoil surface at certain specified points are equal to the inclinations of the velocity vectors lying in the plane $\bar{z} = 0$ but at the same values of the $\bar{x}$ and $\bar{y}$ coordinates of the points. The validity of this assumption cannot be challenged if all the points in the airfoil surface are close to the horizontal plane through the origin (i.e., if the wing is at small angle of attack). It will be true, however, that at fairly large α^2 (barring the occurence of flow separation) the tangent to the wing at any given point (especially if the point is near the tip) may exceed by a finite amount the downwash angle at the corresponding point in the horizontal plane. This line of reasoning infers that the load distribution as computed by the methods of Weissinger, Falkner and Mutterperl will underestimate the true magnitude of the circulation about a highly

swept wing at large α^s . It is borne out by the greater lift curve slope exhibited by the experimental wing.

Result (c) is in a sense misunderstood. Discussed on page 9 of Reference (1) is an effect which causes some differences between theoretical and experimental values of downwash. This is the effect of decreased dynamic pressure in the wake. Within the wake the longitudinal velocity increases as one travels downstream. This requires a vertical flow into the wake. The downwash immediately above is supposedly increased thereby, while below the wake it is decreased. It would, therefore, be expected that for a comparison in which there was agreement between theory and experiment everywhere else, in the region of the wake the experimentally determined downwash would be greater. But in the present case, even though the calculated values outside the wake are somewhat smaller the calculated values within the wake are actually about equal. Further study is required to find the explanation for this. It would seem, however, that since the prediction of the position of the wake depends upon the calculated downwash values along the surface through the center of the wake, and since that in this case this prediction proved to be correct, that these wake values of downwash were actually correct.

CONCLUSIONS

The foregoing analysis shows:

(1) that the Prandtl lifting line theory together with the stepwise circulation approximation to the circulation distribution provides an adequate means for computing the fields of flow behind highly swept wings.

(2) that by taking into consideration the actual orientation of the lifting line (which encloses the trailing vortex origins) and the geometrical displacement of the trailing vortices, it is possible to predict accurately the center of the vortex sheet (and wake) for regions extending reasonably far downstream.

(3) that downwash may be computed over a wide area in the locality of the tail with only a moderate amount of effort, thus avoiding large errors which are the consequence of assuming the downwash to be constant along the horizontal stabilizer span equal to the value at the center.

APPENDIX A

EXAMPLE IN THE USE OF THE METHOD

The following description of a computation is presented to illustrate the method used for finding the downwash behind a given swept wing at moderately high angle of attack.

Description of the Wing:

The following data give the necessary information relative to the wing investigated:

$$\varphi = 45^{\circ}$$

$$C_L = 0.71$$

$$dC_L/d\alpha = 0.047 \text{ (theoretical)}$$

$$AR = 3.64$$

$$\lambda = 0.418$$

$$\text{mac} = 0.592\ b/2$$

$$\alpha = 15.1^{\circ} \text{ (from theoretical } dC_L/d\alpha \text{)}$$

Approximation to Circulation Distribution:

Figure (10) shows the theoretical span loading as computed by the Weissinger Method and reproduced from Figure (2), Reference (3). Superimposed upon the theoretical curve is the stepwise approximation made for the purposes of this investigation.

The values of the function

$$k = k(\bar{s}) = (\tfrac{1}{4}\pi)\,\Delta(2\Gamma/bV) = (C_L/4\pi AR)\,\Delta(C_l c_{\bar{s}}/C_L c_{av})$$

are tabulated below.

$\bar{s}$	$(C_l c_{\bar{s}}/C_L c_{av})$	k
0.500	.10	.001554
0.654	.13	.002015
0.73	.21	.003265
0.92	.29	.00451
1.00	.44	.00683

Determination of Vortex Sheet Distortion:

In this step the downwash is computed along the streamlines lying in the planes $\bar{y} = 0$, $\bar{y} = 0.83$, and $\bar{y} = 0.86$. These planes are chosen to lie midway between the planes containing the adjacent trailing vortices. Along each of the streamlines, the values of w existing at the trailing edge (see Equations 13), at the plane $\bar{x} = 2.75$ and at one point midway between are found. The height of each vortex is assumed to be given by the expression for $\bar{z}$ of the filament coming off the trailing edge. This gives nine points, designated ①, ②, - - ⑨.

Downwash Points	$\bar{x}$	$\bar{y}$	$\bar{z}$
①	0.575	0	-0.155
②	1.66	0	-.155
③	2.75	0	-0.155
④	1.098	.83	-0.298
⑤	1.975	.83	-0.298
⑥	2.75	.83	-0.298
⑦	1.181	.96	-.319
⑧	1.870	.96	-0.319
⑨	2.75	.96	-0.319

Next are determined the radial and longitudinal distances $\bar{r}_b$ and $\bar{p}$ and the values of $\cos\beta_b$ for each of the points by the use of Equations (8) through (10). Computing Form A is useful for this purpose.

Then, using these geometrical data, it is necessary to calculate separately the contributions at each of the points from the bound Vee vortex and from the trailing vortices to the downwash. Computing Form B provides for the tabular solution of Equation (5). In this solution use is made of the curves of

F_b, Figure (8). Similarly, Computing Form C serves as a tabular solution of Equation (7) in which values of F_t from Figure (9) must be entered. On Figure (9) is plotted an auxilliary diagram by which the cosine of the angle β_t and the radius $\bar{r}_t$ may be read directly, using as arguments $\bar{m}$ and Δz ($= \bar{z}_{\text{downwash point}} - \bar{z}_{\text{vortex core}}$). Finally, the downwash angles ϵ_b and ϵ_t are added at each of the nine chosen points in the vortex sheet.

Next, a plot of ϵ versus $\bar{x}$ for each of the three streamlines is prepared. According to Equation (12) the vertical position of any point along a streamline is given by the algebraic sum of the position of the vortex origin plus the integral of the downwash angle from the vortex origin to that point. For purposes of finding induced velocities, the "origin" of a trailing vortex is assumed to extend all the way up to the quarter chord line, but for finding the shape of this filament, the term "origin" refers to the point at which the streamline containing the filament leaves the wing. Therefore, the integration of Equation (12) is started at the trailing edge. An approximate integration formula is given by

$$\int_0^{x_n} f(x)\,dx = \frac{\Delta}{2}(f_0 + f_n) + \Delta \sum_{\nu=1}^{n-1} f_\nu$$

where there are n equally spaced intervals of length Δ between $\bar{x} = 0$ and $\bar{x} = \bar{x}_n$. Figure (11) shows the plots of downwash along the three streamlines. The integration procedure for this example yeilds the following values of $\bar{z}$ at the plane $\bar{x} = 2.08$ (the plane in which experimental data were taken):

@ $\bar{y} = 0$, $\bar{z} = -.155 - .160 = -.315$

@ $\bar{y} = 0.83$, $\bar{z} = -.298 - .105 = -.403$

@ $\bar{y} = 0.96$, $\bar{z} = -.319 - .079 = -.398$

These values of $\bar{z}$ are plotted in Figure (12), and define the

intersection of the vortex sheet with the plane $\bar{x} = 2.08$.

Final Computation of Downwash in Plane of Interest:

The final shape of the vortex pattern is as assumed in Figure (13). Use is again made of Computing Forms A, B and C. For this example the plane of interest is far enough behind the lifting line that the latter's downwash contribution is small compared to that from the trailing vorticity. w_b is therefore assumed to be a function only of $\bar{y}$ (independent of $\bar{z}$) and is obtained by interpolating between values already computed in the preceding step. This distribution of w_b is shown in Figure (14).

In this last step the values of w_t are computed in the plane of interest along the lines $\bar{z} = -0.2$, -0.4 and -0.6. This provides a straddle of the vortex sheet. w_b is found by the method described above. Finally, the separate contributions to the total downwash strengths at points along these lines are added. They have been plotted in Figure (15).

REFERENCES

1. Silverstein, Abe, Katzoff, S., and Bullivant, W. Kenneth: Downwash and Wake Behind Plain and Flapped Airfoils. T.R. No. 651, N.A.C.A., 1939.

2. Silverstein, Abe, and Katzoff, S.: Design Charts for Predicting Downwash Angles and Wake Characteristics Behind Plain and Flapped Airfoils. T.R. No. 648, N.A.C.A., 1939.

3. Van Dorn, Nicholas H., and DeYoung, John: A Comparison of Three Theoretical Methods of Calculating Span Load Distribution on Swept Wings. T.N. No. 1476, N.A.C.A., 1947.

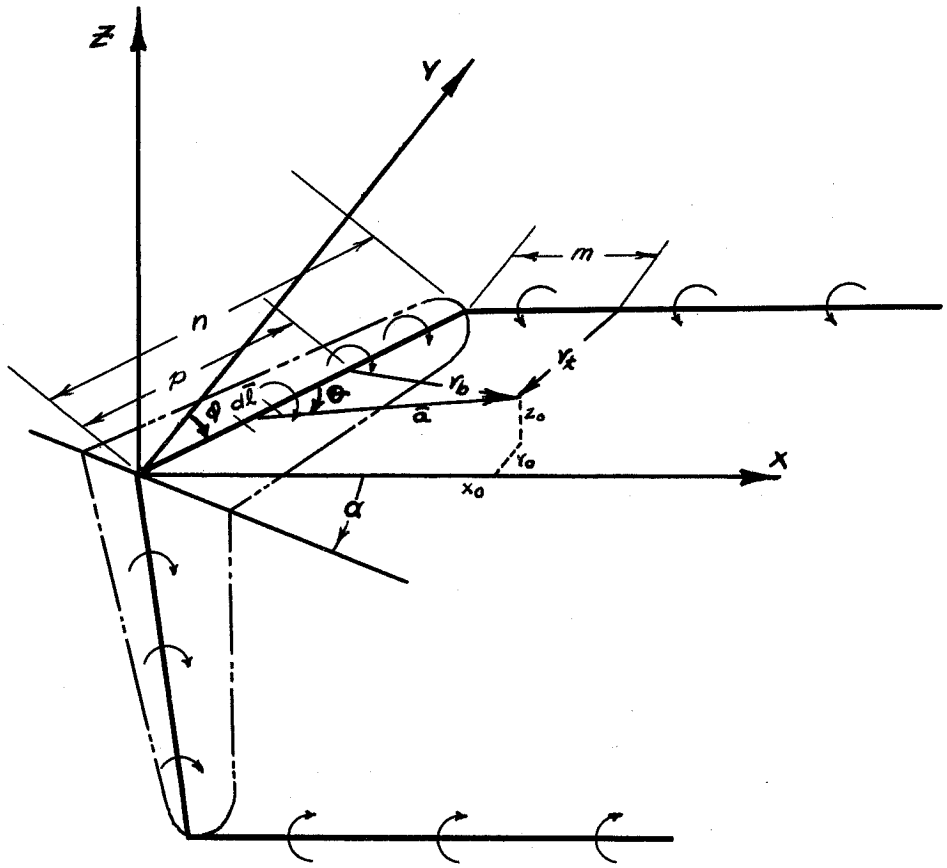

Figure (1) - Horseshoe Vortex with Vee Lifting Line

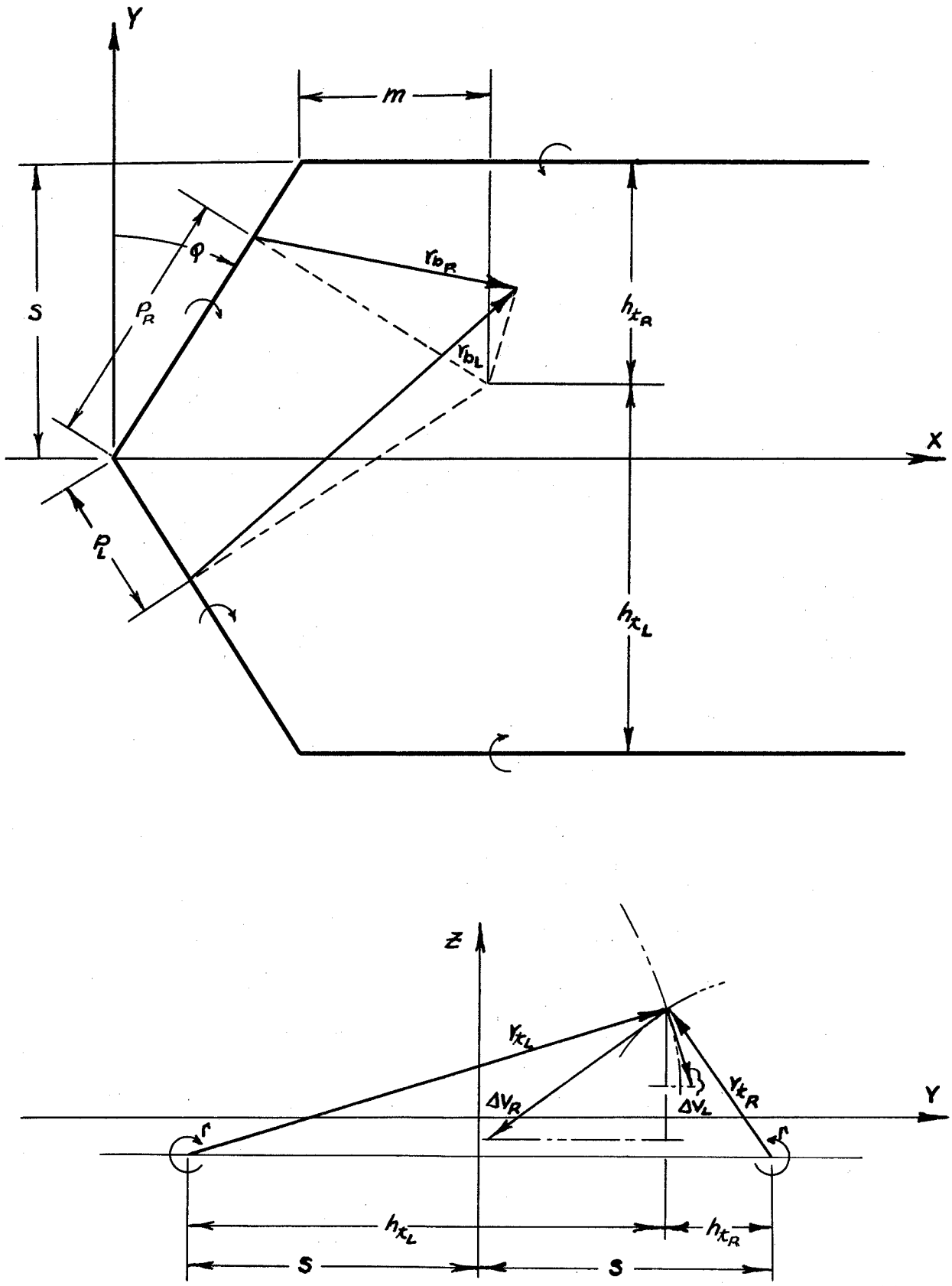

Figure (2) - Geometrical Quantities Involved in Determination of Downwash Induced by Vee Vortex of Strength Γ.

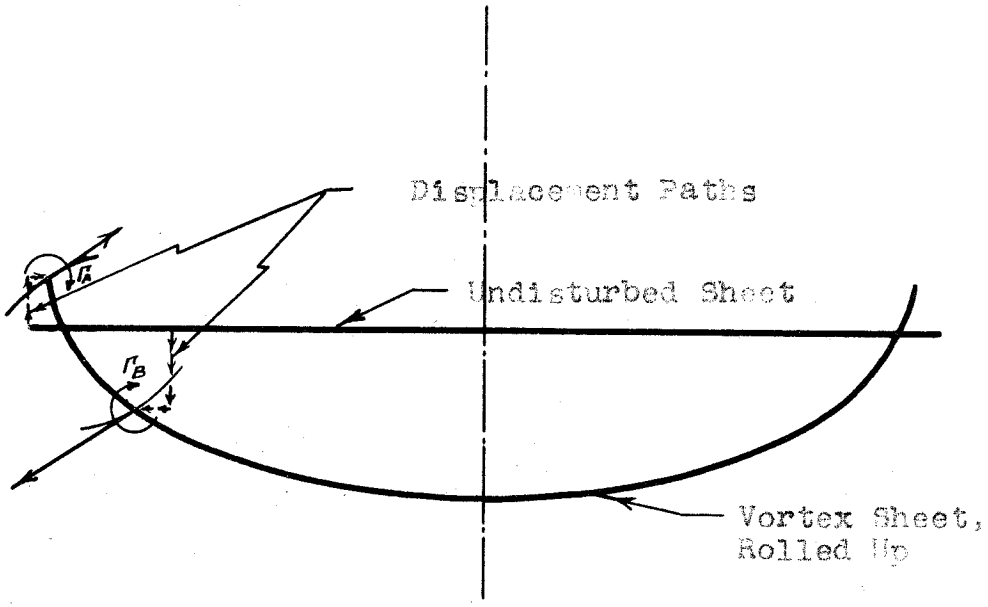

Figure (3) - Distortion of Vortex Sheet Showing Displacement of Each of Two Vortices by The Other; Vortex Cores Located Near Edge of The Sheet. Magnitudes of Velocity Vectors Plotted Proportional to Vortex Strengths.

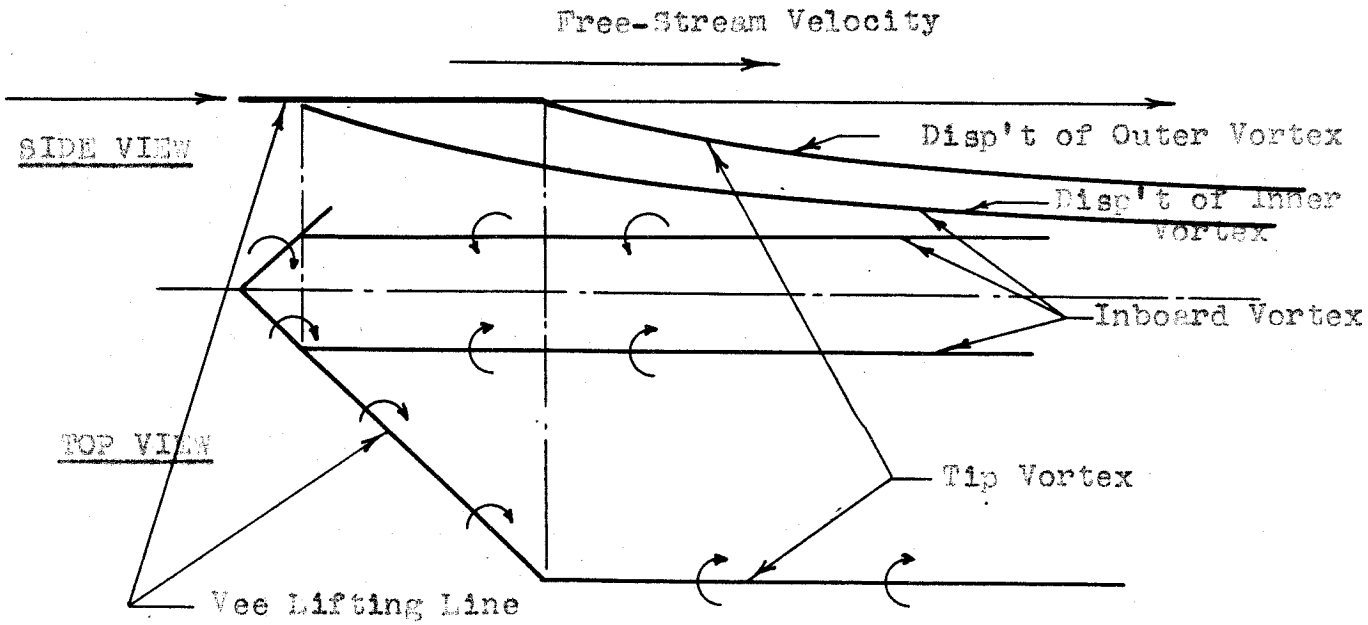

Figure (4) - Simplified Vortex System for Highly Swept Wing at Zero Angle of Attack - Illustrating Relative Displacement of Inner and Outer Trailing Vortices as a Function of Downstream Distance.

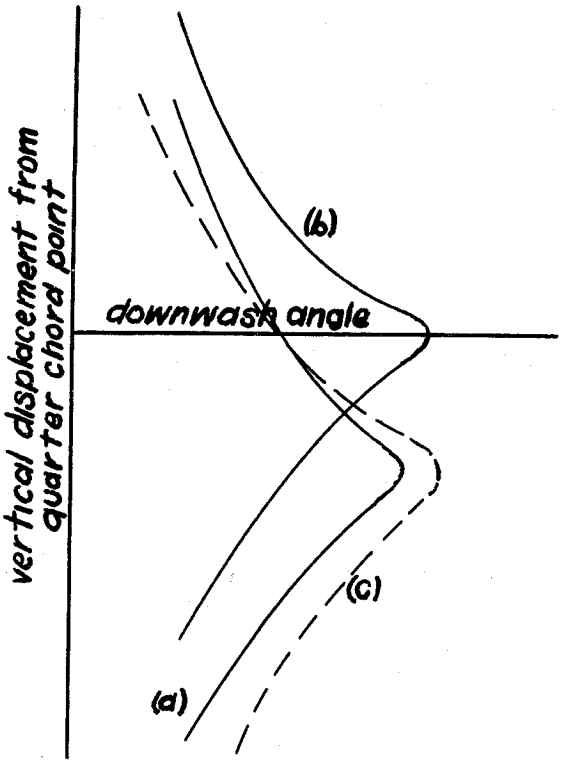

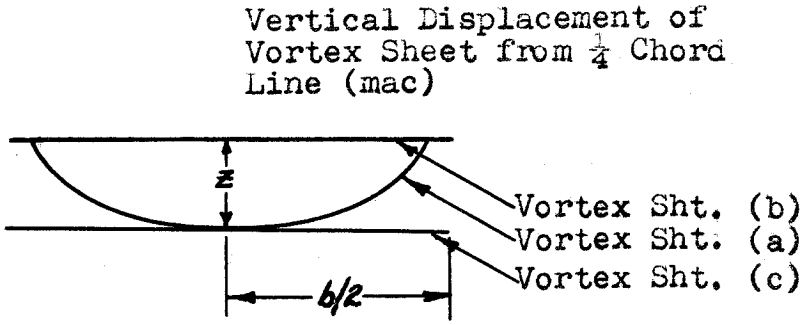

Figure (5) - Calculated downwash for the plane of symmetry, 1.15 semispans behind the quarter-chord line of a 2:1 tapered airfoil of aspect ratio 6. C_L, 1.35. a, Vortex sheet distorted as found for the U.S.A. 45 tapered airfoil; b, Vortex sheet assumed to extend unchanged straight behind the quarter-chord line to infinity; c, same as b, but displaced vertically by an amount equal to the displacement at the middle of the distorted sheet. (Figure 12 from Ref. 1)

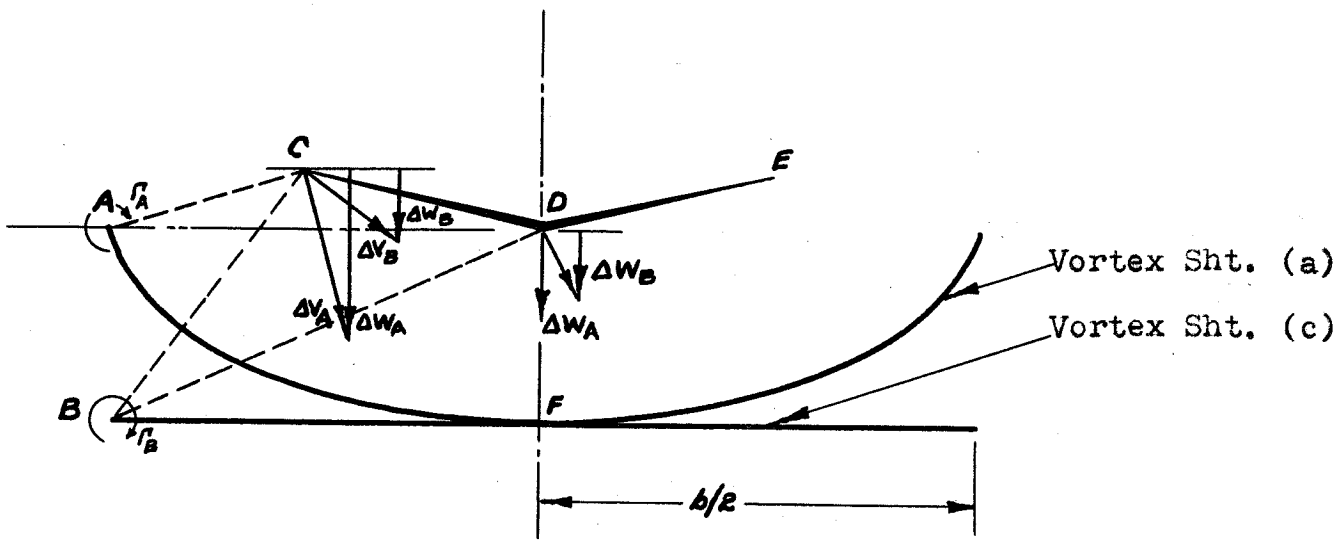

Figure (6) - Comparison of downwash induced along the horizontal tail by a plane vortex sheet (vortex sht. c) and by a curved vortex sheet (vortex sht. a) behind a fictitious wing. Induced tangential velocities plotted inversely proportional to distance from vortices.

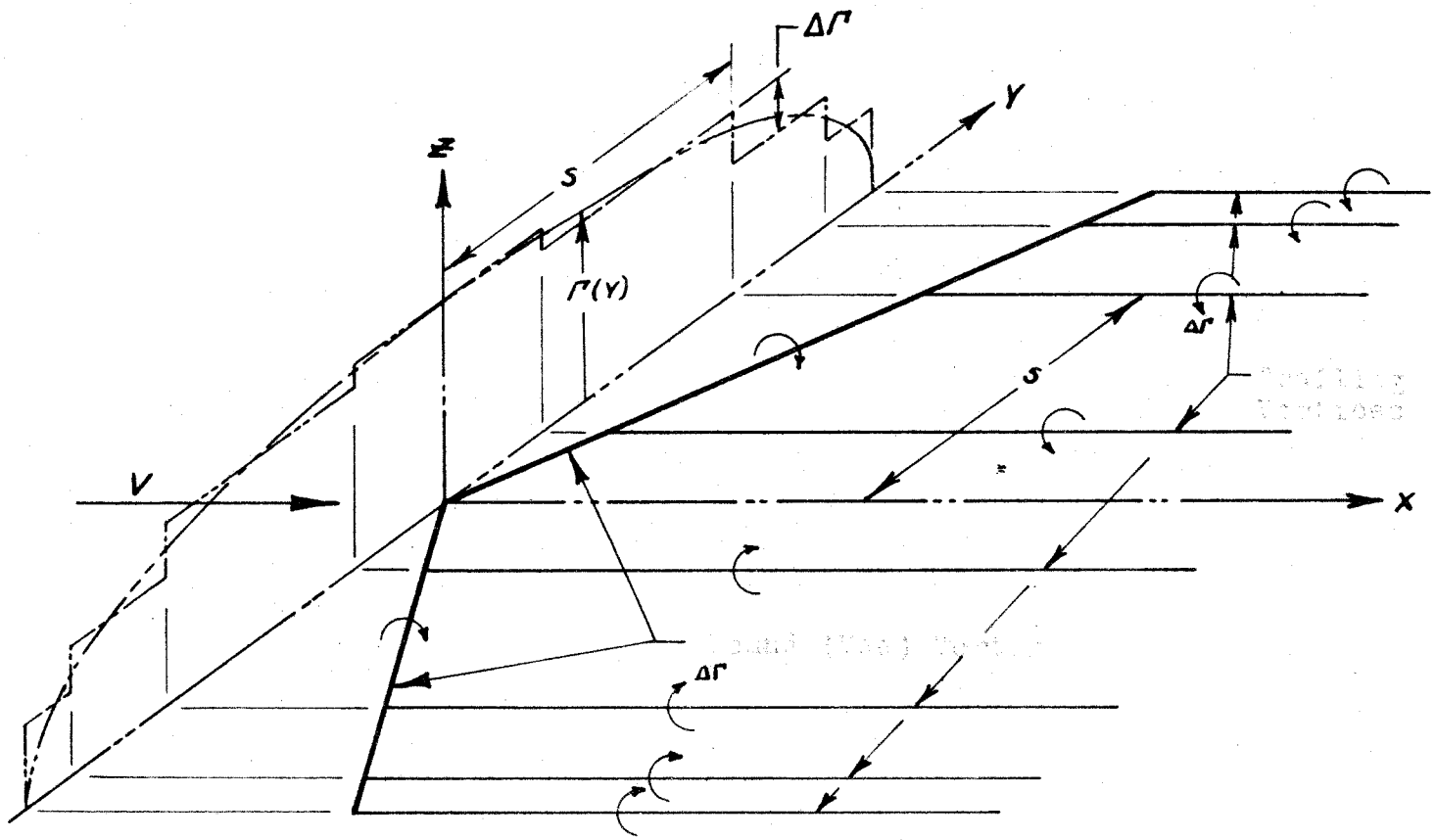

Figure (7) - Theoretical Span Load Distribution $\Gamma(y)$ and Equivalent Stepwise Distribution (showing assumed bound and trailing vortex pattern).

FIGURE (8) - INDUCED VELOCITY FUNCTION, F_b, DUE TO VORTEX FILAMENT OF UNIT LENGTH (BOUND VORTEX)

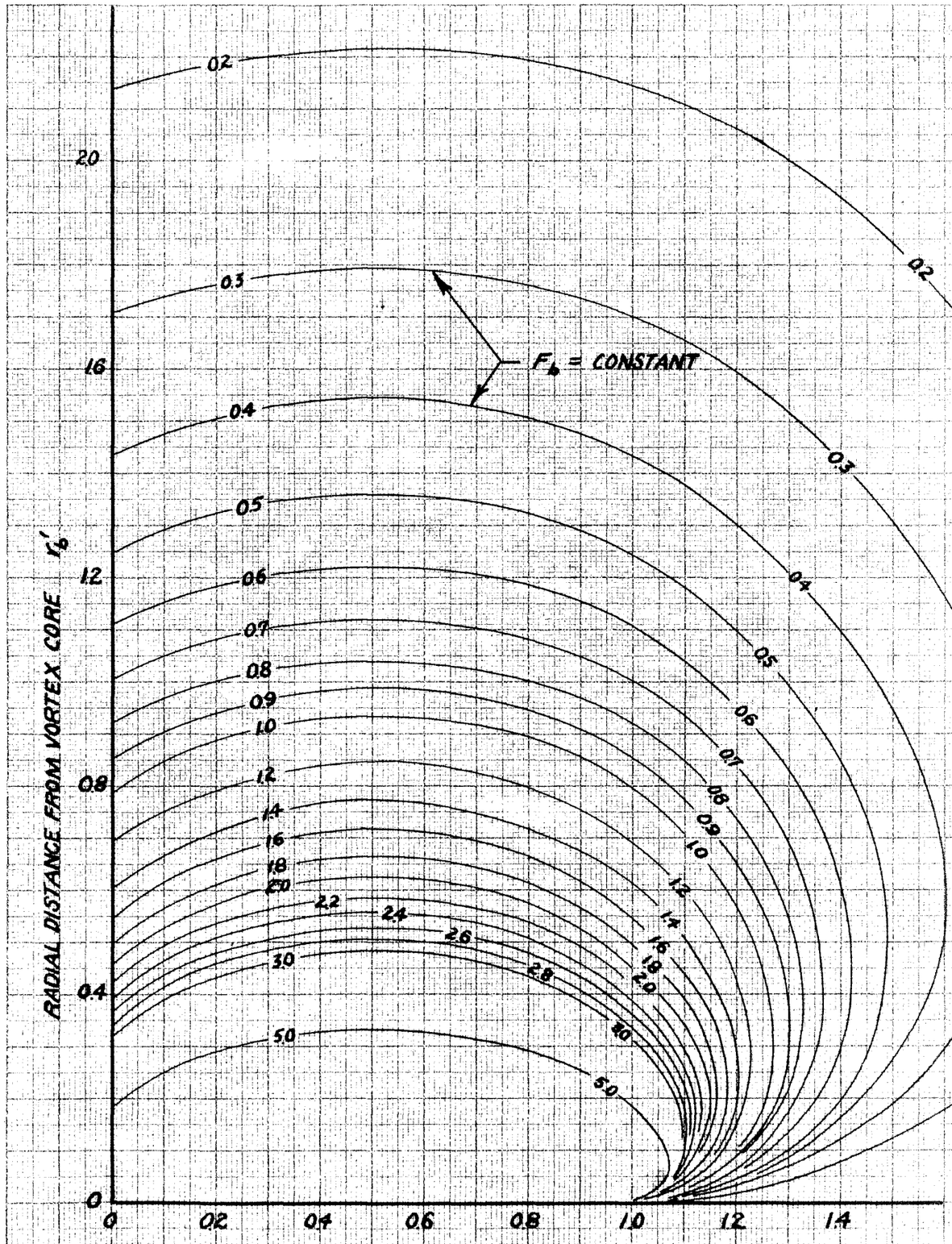

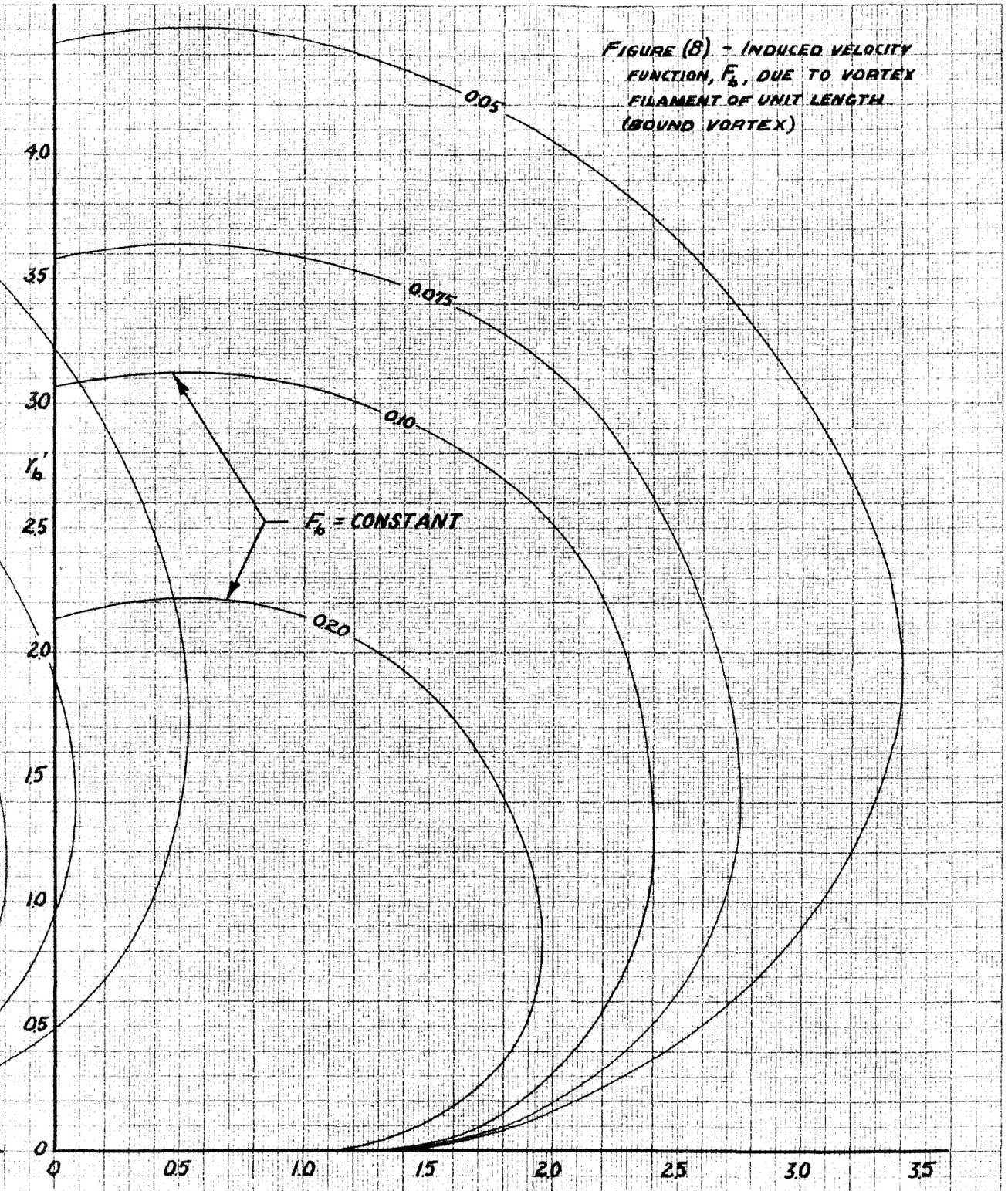

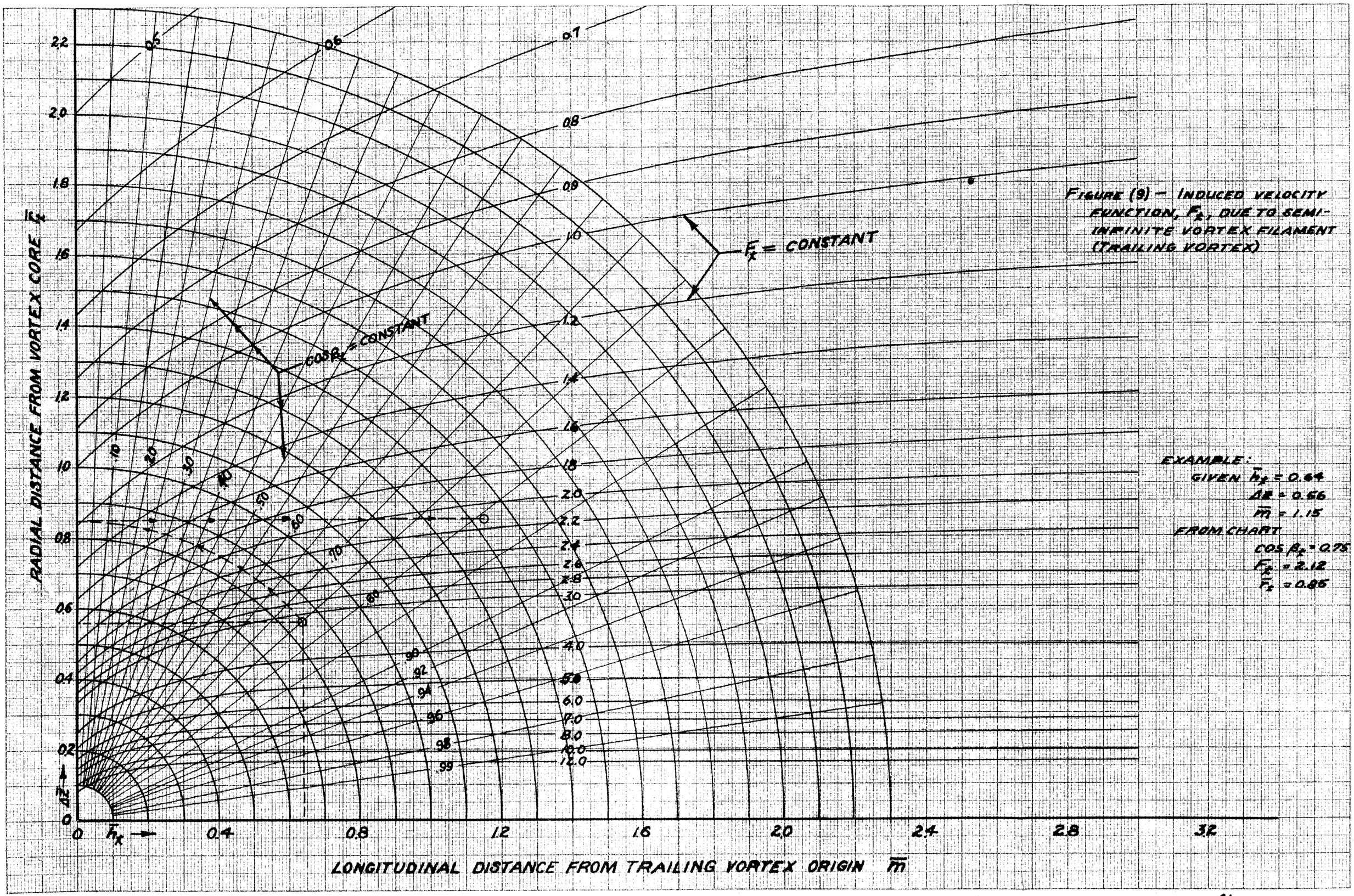

FIGURE (9) — INDUCED VELOCITY FUNCTION, F_x, DUE TO SEMI-INFINITE VORTEX FILAMENT (TRAILING VORTEX)

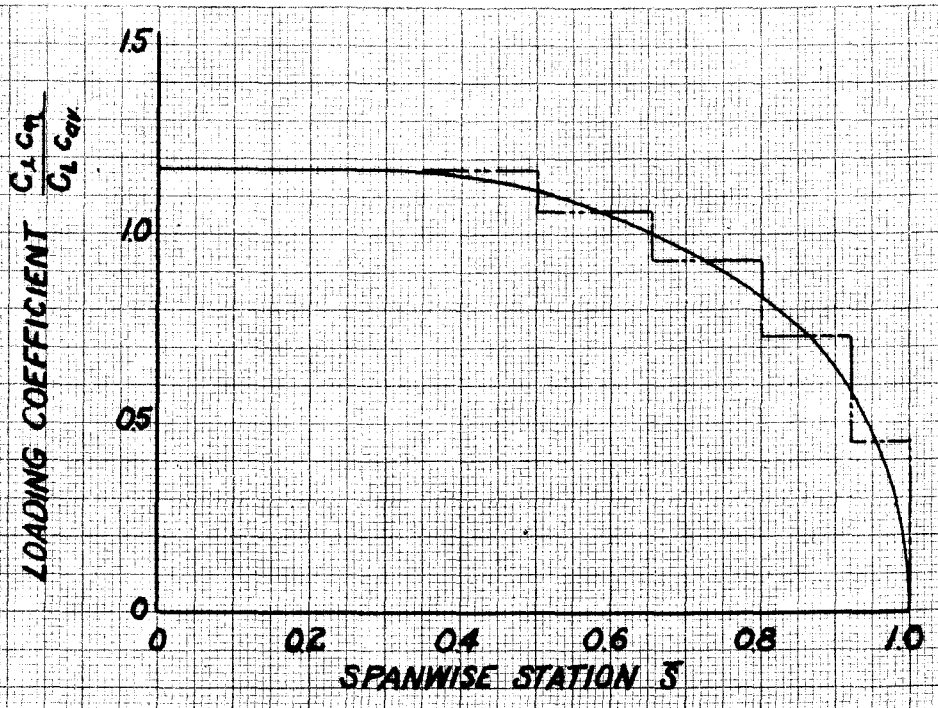

Figure (10) - Theoretical and Approximate Spanwise Circulation Distribution for an Untwisted Wing with 45° Sweepback. (See Figure 2, Reference 3)

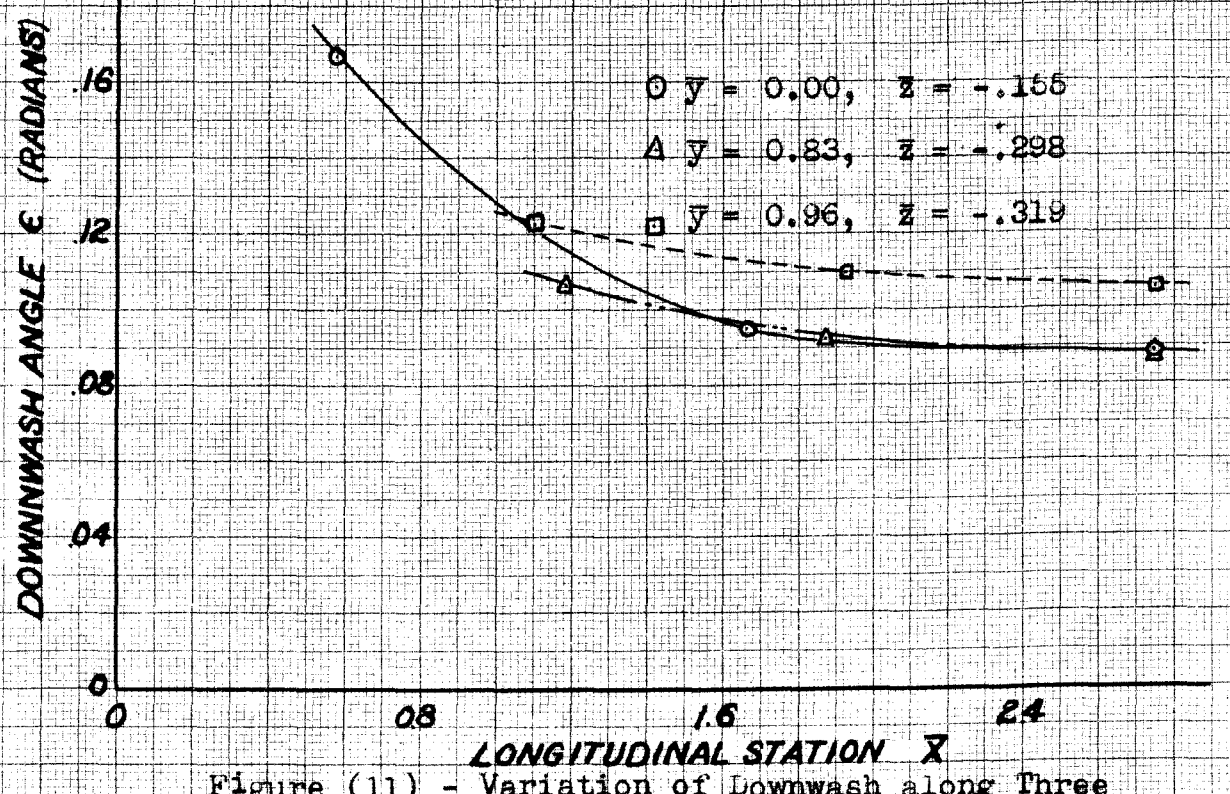

Figure (11) - Variation of Downwash along Three Selected Undistorted Streamlines in the Trailing Vortex Sheet

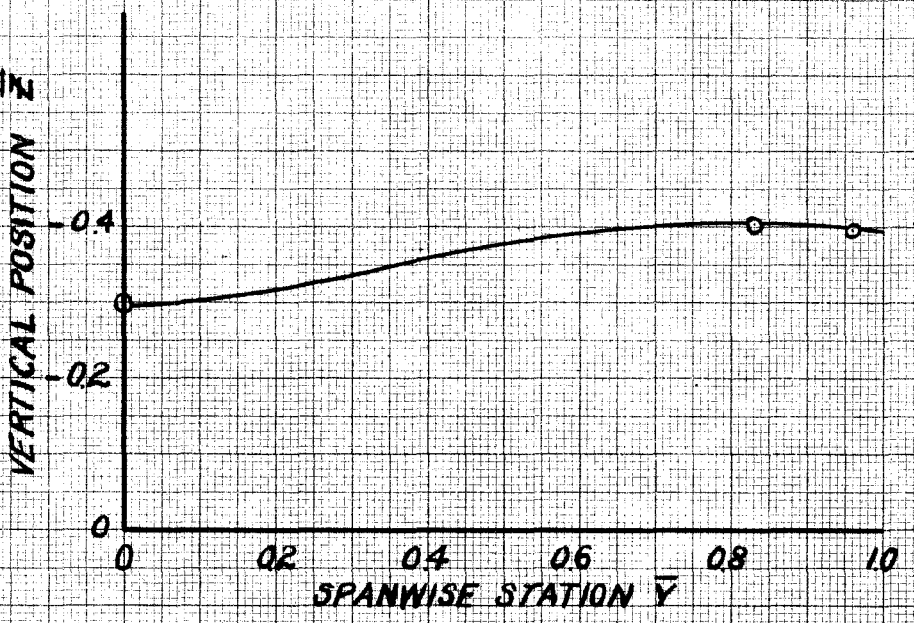

Figure (12) - Intersection of the Trailing Vortex Sheet with the Plane $\bar{x} = 2.08$

Figure (13) - Distorted Shape of the Vortex Pattern as Assumed for Use in Making Final Downwash Calculations

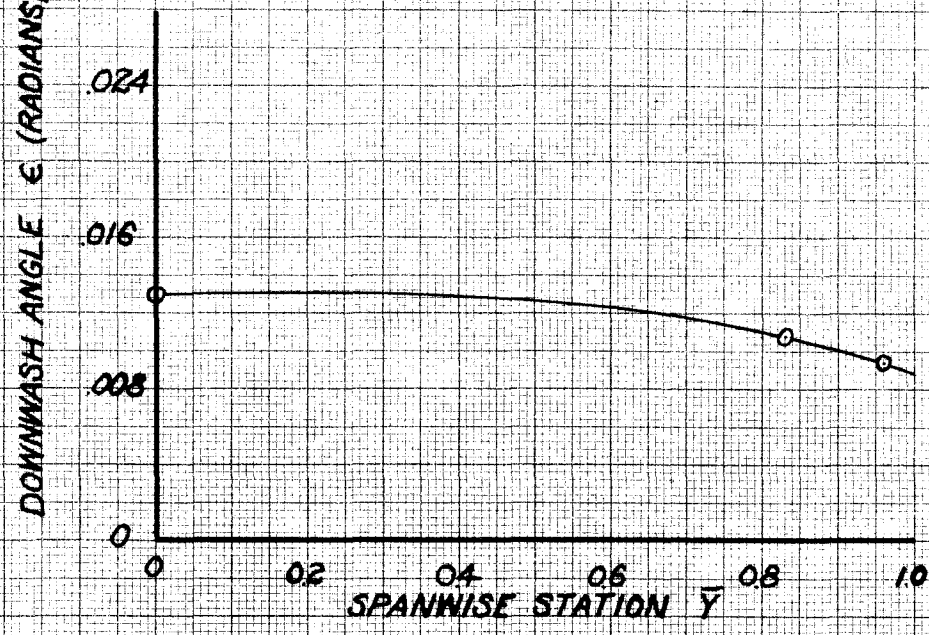

Figure (14) - Spanwise Variation of Downwash from the Vortices Bound to the Lifting Line in the Plane $\bar{x} = 2.08$.

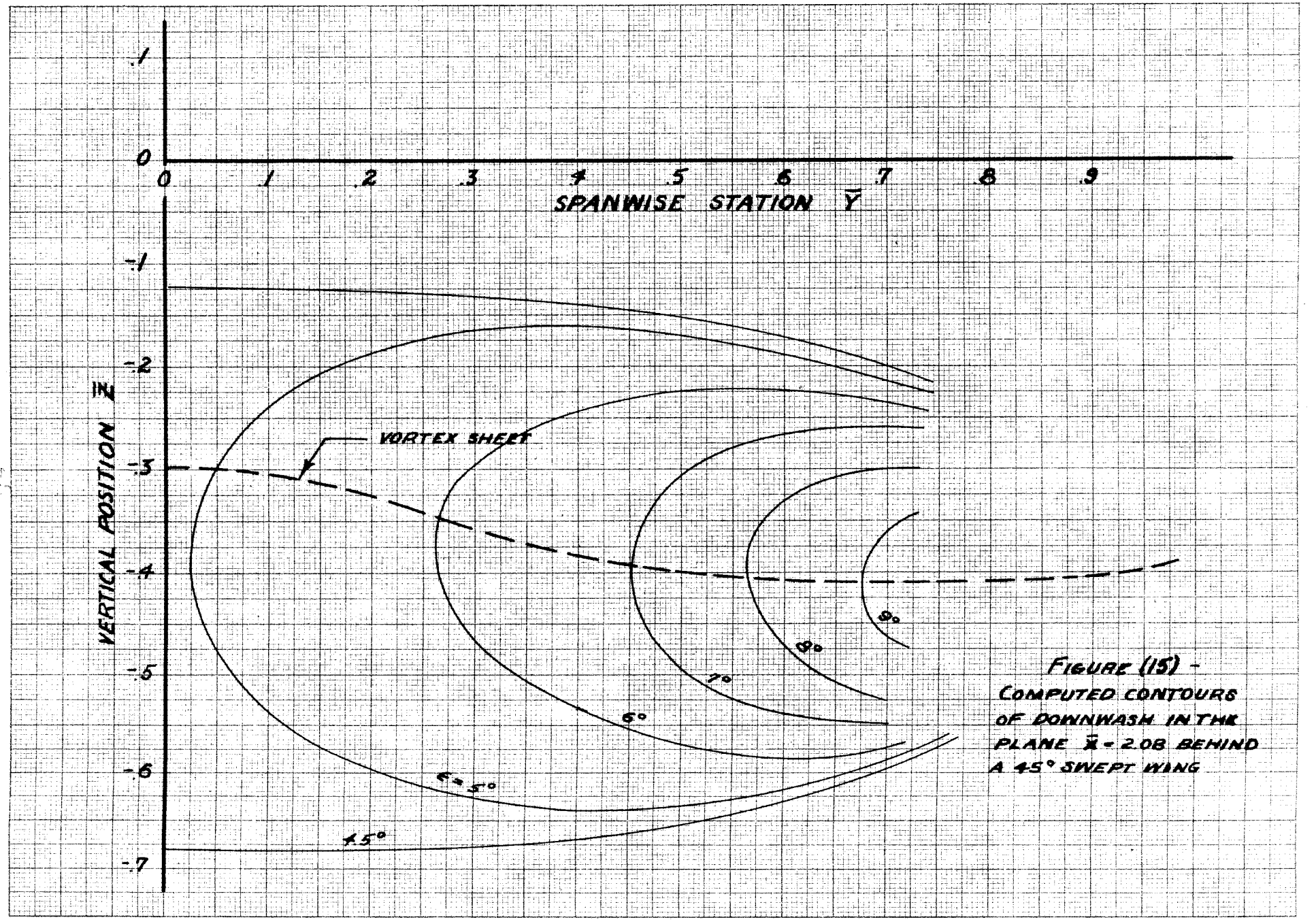

FIGURE (15) - COMPUTED CONTOURS OF DOWNWASH IN THE PLANE $\bar{X} = 2.08$ BEHIND A 45° SWEPT WING

Computing Form A - Solution of Equations (8) through (10) for Determination of the Radial and Longitudinal Lengths $\bar{r}_b$ and $\bar{p}$ and for the Cosine of the Angle β_b.

	(1)	(2)	(3)	(4)	(5)	(6)	(7)	(8)	(9)	(10)	(11)	(12)	(13)	(14)	(15)	(16)	(17)	(18)	(19)
DOWN-WASH PT.	$\bar{X}$	$\bar{Y}$	$\bar{Z}$	$\bar{X}\cos\alpha$	$\bar{X}\sin\alpha$	$\bar{Z}\cos\alpha$	$\bar{Z}\sin\alpha$	$\bar{Y}\sin\varphi$	$\bar{Y}\cos\varphi$	(4) − (7) K	(10)$\cos\varphi$	(10)$\sin\varphi$	(11)−(8)^2	(5)+(6)^2 f^2	$\sqrt{(13)+(14)}$ $\bar{r}_{b_R}$	(9)+(12) $\bar{p}_R$	$\sqrt{(11)+(8)^2}$	$\sqrt{(17)+(14)}$ $\bar{r}_{b_L}$	(12)−(9) $\bar{p}_L$
(1)																			
(2)																			
(3)																			
(4)																			
(5)																			

	(20)	(21)	(22)	(23)	(24)	(25)	(26)	(27)	(28)	(29)	(30)	(31)	(32)	(33)
DOWN-WASH PT.	(16)$\cos\varphi$ $\bar{p}_R\cos\varphi$	(15)$\cos\varphi$ $\bar{f}_{b_R}\cos\varphi$	(19)$\cos\varphi$ $\bar{p}_L\cos\varphi$	(18)$\cos\varphi$ $\bar{f}_{b_L}\cos\varphi$	(2)−(20)	(24)^2	(16)$\sin\varphi$	(19)$\sin\varphi$	(26)$\cos\alpha$	(29)$\cos\alpha$	(1)−(28)	(30)^2	(25)+31)	$\sqrt{(32)}$
(1)														
(2)														
(3)														
(4)														
(5)														

	(34)	(35)	(36)	(37)	(38)	(39)	(40)	(41)
DOWN-WASH PT.	(2)+(22)	(34)^2	(1)−(29)	(36)^2	(25)+(37)	$\sqrt{(38)}$	(33)/(15) $\cos\beta_{b_R}$	(39)/(18) $\cos\beta_{b_L}$
(1)								
(2)								
(3)								
(4)								
(5)								

DOWNWASH DUE TO THE BOUND VORTEX

DOWNWASH POINT ◯ $K = (1/4\pi)(2\Gamma/bV)$

①	②	③	④	⑤	⑥	⑦	⑧	⑨	⑩	⑪
$\bar{s}$	$\bar{r}_{b_R}\cos\phi$ r'_{b_R}	$\bar{p}_R\cos\phi$ p'_R	F_{b_R} FIG 8	$\bar{r}_{b_L}\cos\phi$ r'_{b_L}	$p_L\cos\phi$ p'_L	F_{b_L} FIG 8	$K\cos\phi$	⑧/①	④×⑨ $\Delta(w/v)_{b_R}$	⑦×⑨ $\Delta(w/v)_{b_L}$
									$\sum$	$\sum$

$$(w/V)_b = \cos\beta_{b_R}\sum\Delta(w/V)_{b_R} + \cos\beta_{b_L}\sum\Delta(w/V)_{b_L} = \_\_\_\_\_$$

Computing Form B - Solution of Equation (5) for Downwash Induced at a Given Point by the Bound Vortex

DOWNWASH DUE TO TRAILING VORTICES

$\Delta z = z_{downwash\ pt.} - z_{vortex\ core}$ $\quad K = (1/4\pi)(2\Gamma/b_v)$

DOWNWASH POINT ◯

$\bar{x} =$ ____
$\bar{y} =$ ____
$\bar{z} =$ ____

①	②	③	④	⑤	⑥	⑦	⑧	⑨	⑩	⑪	⑫	⑬	⑭	⑮
Δz	$\bar{s}$	$\bar{s}\tan\theta \times \cos\alpha$	$\bar{x} - ③$	$\bar{s} - \bar{y}$	$\cos\beta_{x_R}$	F_{x_R}	⑥×⑦	$\bar{s} + \bar{y}$	$\cos\beta_{x_L}$	F_{x_L}	⑩×⑪	⑧+⑫	K	⑬×⑭
		$\bar{m}$		$\bar{h}_{x_R}$	FIG 9	FIG 9		$\bar{h}_{x_L}$	FIG 9	FIG 9				$\Delta(w/v)_x$

$(w/v)_x = \sum \Delta(w/v)_x = $ ____

Computing Form C - Solution of Equation (7) for Downwash Induced at a Given Point by the Trailing Vortices